Investigation of Thermosphere Mass Density Perturbations Ascribed by CHAMP Observations

Anton Buynovskiy[1], Jeffrey P. Thayer[1,2], Eric K. Sutton[2]

[1]CU Boulder/Aerospace Engineering Science, [2]CU Boulder/SWxTREC; Corresponding Author: anton.buynovskiy@colorado.edu

Motivation

- CHAMP accelerometry has provided a decade's worth of drag acceleration data, yet in-track wind influences on acceleration are often neglected
- A new ascending-descending accelerometry (ADA) technique has been developed and demonstrated that the in-track wind perturbations can be extracted and analyzed
- This poster applies the ADA technique to CHAMP accelerometer data in the high-latitude region to reveal potential in-track wind contributions

General Accelerometry

- Highly sensitive accelerometers, such as STAR on the CHAMP mission, have been used to extract thermosphere properties such as mass density and cross-track winds by relating the acceleration due to drag to density and wind [1] as shown below

$$\boldsymbol{a}_d = -\frac{\rho}{2m} C_d A |\boldsymbol{v}| \boldsymbol{v} \quad (1)$$

where $\boldsymbol{a}_d$ is the drag acceleration, C_d is the drag coefficient, A is the reference area, m is the spacecraft mass, ρ is the thermospheric mass density, $\boldsymbol{v} = \boldsymbol{v}_{sc} - \boldsymbol{v}_{corot} - \boldsymbol{v}_{wind}$ is the relative velocity of the atmosphere with respect to the satellite, $\boldsymbol{v}_{sc}$ is spacecraft velocity, $\boldsymbol{v}_{corot}$ is the co-rotating atmospheric wind, and $\boldsymbol{v}_{wind}$ is the thermospheric wind

- An ambiguity between mass density and winds makes it difficult to distinguish mass density and wind perturbations
  - This is typically resolved by either neglecting winds or modeling the winds and absorbing the wind effect as a contributing error

Ascending-Descending Accelerometry (ADA)

ADA splits satellite orbits into ascending and descending passes to take advantage of the fact that while mass density is scalar, winds have a directionality with respect to the relative satellite motion, making it possible to discern whether acceleration perturbations are due to mass density or wind changes. See Buynovskiy et al. (2024) for a detailed procedure.

Conditions

1. Satellite must ascend and descend through the same local time with similar space environment conditions
2. Orbit must be near polar to mitigate in-track contributions from large co-rotating atmospheric and zonal winds
3. Target region should be a persistent, recurring phenomenon

Interpretation

a) Density-dominated: acceleration perturbations due to density are much greater than those due to winds
- Wind perturbations are considered small, so ascending and descending orbits yield similar acceleration perturbations
- The threshold to determine density dominance is shown in Eq. 2a accompanied by density perturbation contributions in Eq. 2b

$$|\Delta a_{rel}| < |a_{rel,asc} + a_{rel,des}| \quad (2a)$$

$$\Delta\rho_{contribution} = \left(1 - \frac{|\Delta a_{rel}|}{2|a_{rel,asc} + a_{rel,des}|}\right) * 100 \quad (2b)$$

b) Wind-dominated: acceleration perturbations due to winds are much greater than those due to density
- Density is considered constant, so the wind perturbations yield an inverse behavior between ascending and descending orbits
- The threshold to determine wind dominance is shown in Eq. 3a accompanied by wind perturbation contributions in Eq. 3b

$$|\Delta a_{rel}| > |a_{rel,asc} + a_{rel,des}| \quad (3a)$$

$$\Delta v_{contribution} = \left(1 - \frac{|a_{rel,asc} + a_{rel,des}|}{2|\Delta a_{rel}|}\right) * 100 \quad (3b)$$

Data Description

- CHAMP in-track accelerometer data from 2003-2006 is used
- The in-track drag accelerometer data is normalized to a constant altitude and put into a relative acceleration format
- The relative accelerations are split into ascending (Fig. 1a) and descending (Fig. 1b) passes, for a total of 8 ADA datasets
  - CHAMP's precession rate allows the satellite to ascend a local time and descend the same local time approximately a year later
- To remove in-track contributions from co-rotating and zonal winds at high latitudes, data with the meridional component <95% are not considered
- Data where Kp > 3 is removed
- Relative accelerations are organized into 1-hour magnetic local time (MLT) and 2° magnetic latitude (mlat) bins

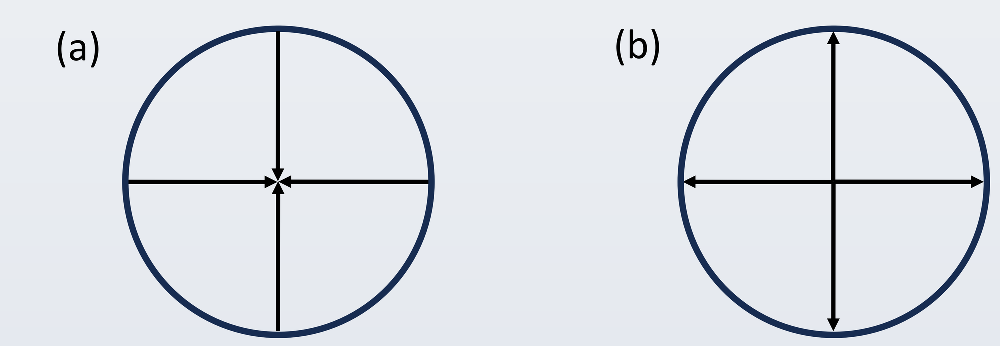

Figure 1: Ascending (a) and descending (b) orbits in the north pole

Results

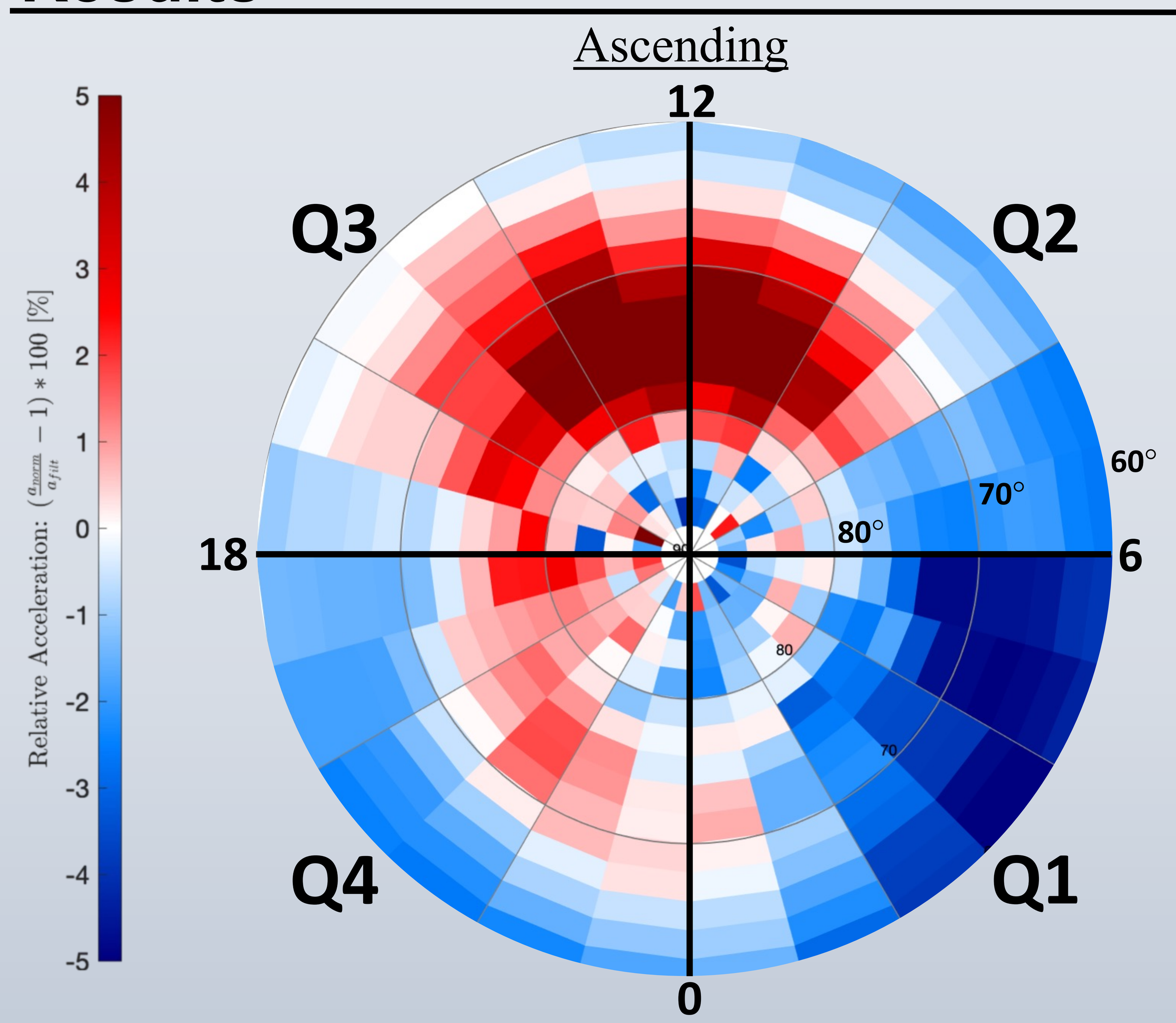

Figure 2: Averaged ascending relative acceleration data in the north pole organized in mlat and MLT

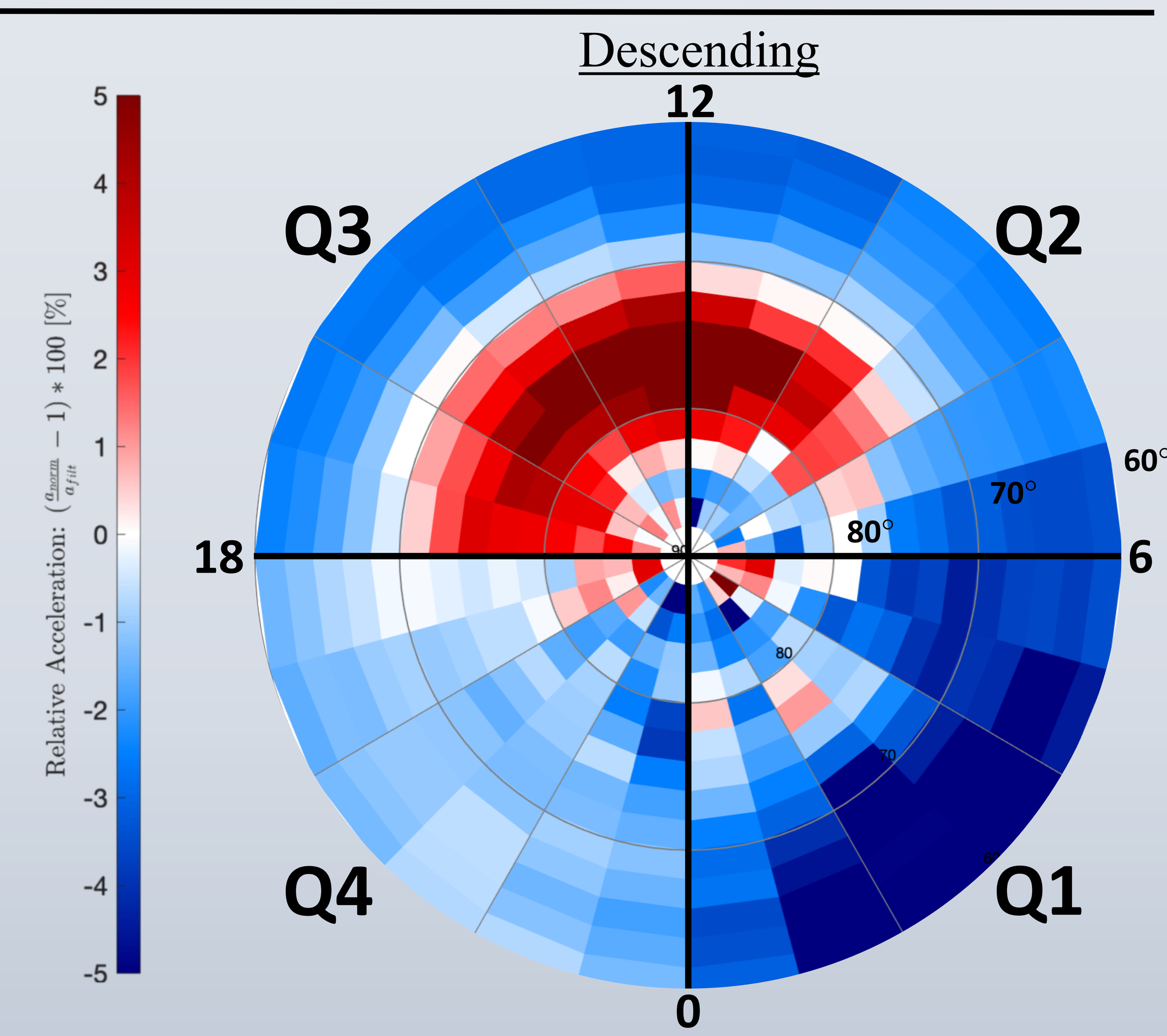

Figure 3: Averaged descending relative acceleration data in the north pole organized in mlat and MLT

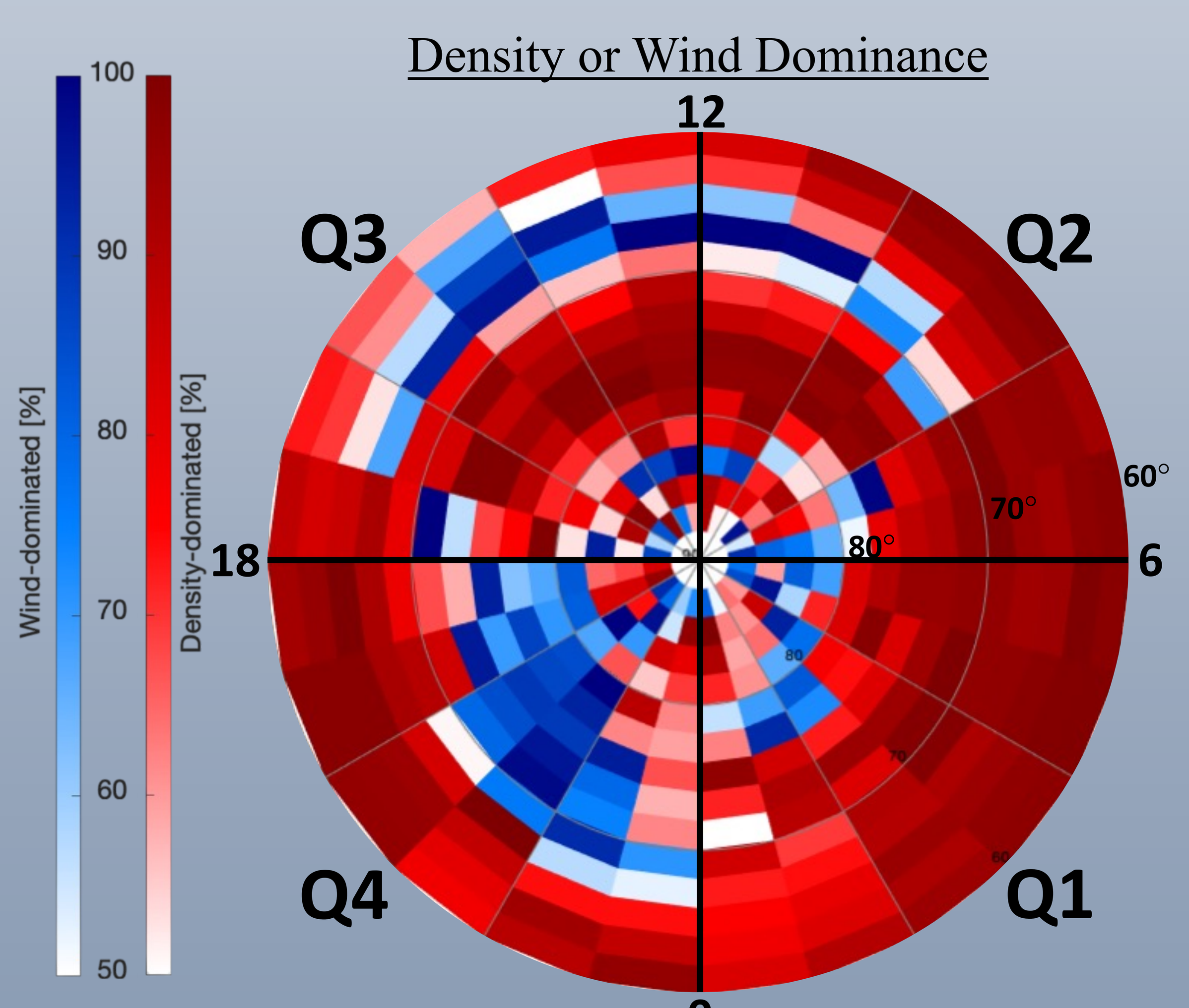

Figure 4: Percent contribution of wind and density perturbations in the north pole organized in mlat and MLT

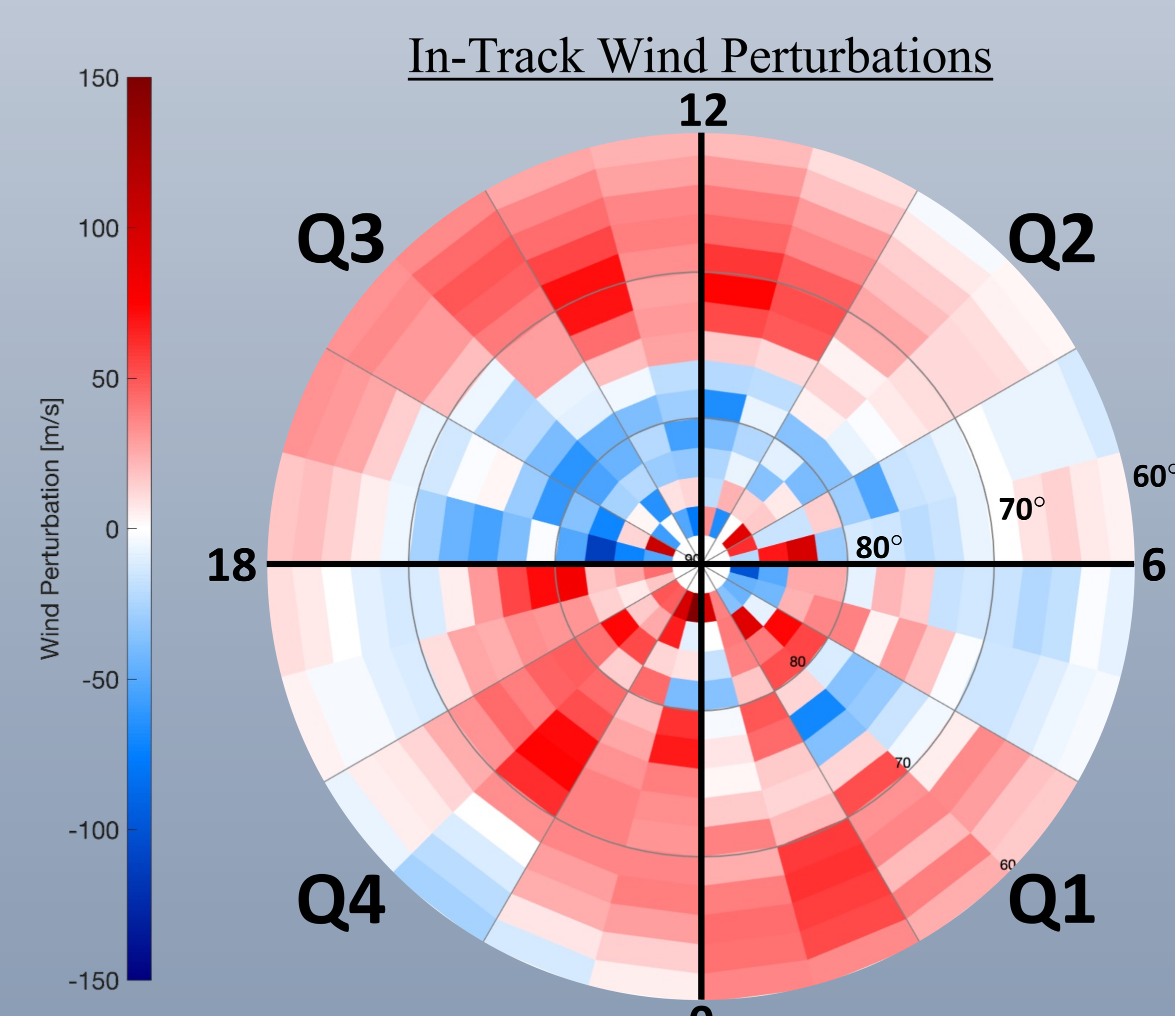

Figure 5: Averaged derived in-track wind perturbations (positive = equatorward, negative =poleward)

Conclusion

Early Morning Quadrant (Q1)

- Ascending (Fig. 2) and descending (Fig. 3) passes both reveal primarily negative acceleration perturbations in this region up to 7%
- Figure 4 shows that this region is primarily density-dominated
- Figure 5 demonstrates that this region primarily has equatorward wind perturbations up to 100 m/s
  - These wind perturbations are consistent with past hybrid wind models as shown in Fig. 7

Dayside Cusp Quadrants (Q2-Q3)

- Ascending (Fig. 2) and descending (Fig. 3) passes both reveal strong positive acceleration perturbations up to 8% at the cusp region
  - This structure is consistent with past observations (see Fig. 6) albeit of different magnitudes
- Figure 4 shows that the cusp is primarily density-dominated with a wind-dominated structure at the lower latitudes
- Figure 5 demonstrates that there are equatorward wind perturbations from 60-76° mlat and poleward wind perturbations from 75-88° mlat up to 115 m/s
  - This indicates a local divergence which is important to recognize for cusp formation mechanisms
  - The poleward wind perturbations are consistent with the day-night wind flow as shown in Fig. 7

Pre-midnight Quadrant (Q4)

- The ascending (Fig. 2) data reveals acceleration perturbation enhancements up to 6% that are not present in the descending (Fig. 3) data
  - This contrasts with the interpretation given in Fig. 6
- Figure 4 shows that a significant portion of this region is wind-dominated
  - Neglecting in-track winds when deriving mass density from accelerometry could result in enhanced/diminished density structures
- Figure 5 demonstrates that this region primarily has equatorward wind perturbations up to 150 m/s
  - The equatorward wind perturbations are consistent with the day-night wind flow as shown in Fig. 7

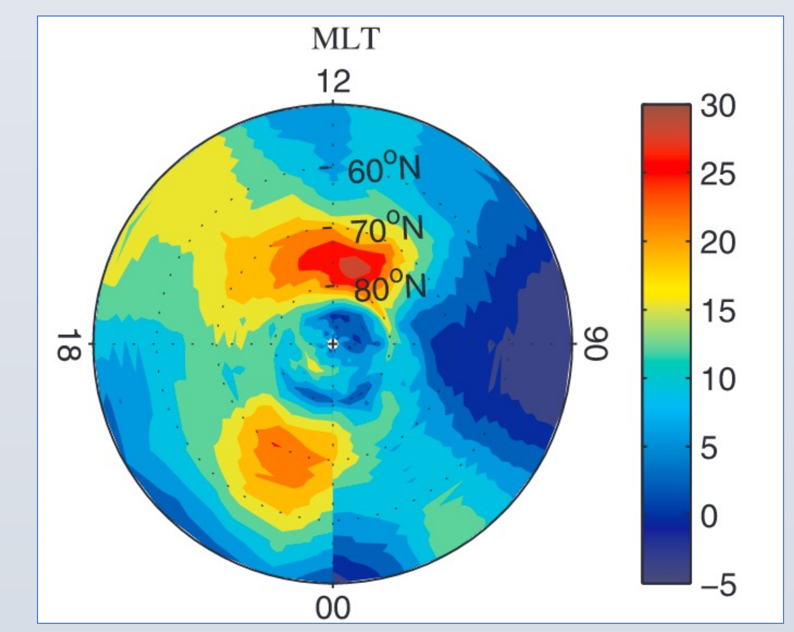

Figure 6: Percent difference between CHAMP-derived mass density and MSIS with in-track winds neglected [3]

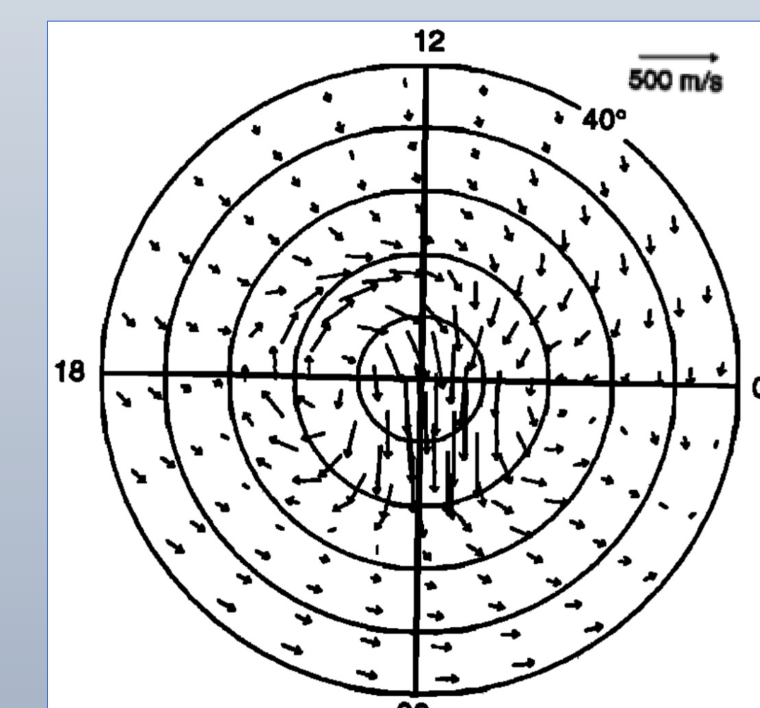

Figure 7: Reconstituted wind fields in geomagnetic coordinates combining DE-2 and TIGCM winds at Kp < 3 [4]

References

1. Sutton, E. K., Nerem, R. S., & Forbes, J. M. (2007). Density and winds in the thermosphere deduced from accelerometer data. *Journal of Spacecraft and Rockets*, **44**, 1210–1219. https://doi.org/10.2514/1.28641
2. Buynovskiy, A., Thayer, J. P., & Sutton, E. K. (2024). Distinguishing density and wind perturbations in the equatorial thermosphere anomaly. *Journal of Geophysical Research: Space Physics*, 129, e2024JA032547. https://doi.org/10.1029/2024JA032547
3. Liu, H., H. Lühr, V. Henize, and W. Köhler (2005), Global distribution of the thermospheric total mass density derived from CHAMP, *J. Geophys. Res.*, 110, A04301, doi:10.1029/2004JA010741.
4. Thayer, J. P., & Killeen, T. L. (1993). A kinematic analysis of the high-latitude thermospheric neutral circulation pattern. *Journal of Geophysical Research*, *98*(A7), 11549. https://doi.org/10.1029/93ja00629

Acknowledgements

This work is based upon work supported by the National Science Foundation Graduate Research Fellowship under Grant DGE 2040434, the National Science Foundation Collaborative Research: CubeSat Ideas Lab: Space Weather Atmospheric Reconfigurable Multiscale Experiment (SWARM-EX) CubeSats under Award No. 1936665, the NASA GDC IDS under Contract No. 80GSFC22CA012, and the NASA Heliophysics Division Space Weather Science Application Initiative under Grant 80NSSC21K1554.